

# A 17-mer Membrane-Active MSI-78 Derivative with Improved Selectivity toward Bacterial Cells

Claudia Monteiro,<sup>†,‡,§</sup> Marina Pinheiro,<sup>§,||</sup> Mariana Fernandes,<sup>†,‡</sup> Sílvia Maia,<sup>⊥</sup> Catarina L. Seabra,<sup>†,‡,‡,¶</sup> Frederico Ferreira-da-Silva,<sup>†,Δ</sup> Salette Reis,<sup>||</sup> Paula Gomes,<sup>⊥</sup> and M. Cristina L. Martins<sup>\*,†,‡,‡</sup>

<sup>†</sup>I3S, Instituto de Investigação e Inovação em Saúde, Universidade do Porto, Porto, Portugal

<sup>‡</sup>INEB, Instituto de Engenharia Biomédica, Universidade do Porto, Rua do Campo Alegre 823, 4150-180 Porto, Portugal

<sup>||</sup>UCIBIO-REQUIMTE, Faculdade de Farmácia, Universidade do Porto, Rua de Jorge Viterbo Ferreira 228, 4050-313 Porto, Portugal

<sup>⊥</sup>UCIBIO-REQUIMTE, Departamento de Química e Bioquímica, Faculdade de Ciências, Universidade do Porto, Rua do Campo Alegre 687, 4169-007 Porto, Portugal

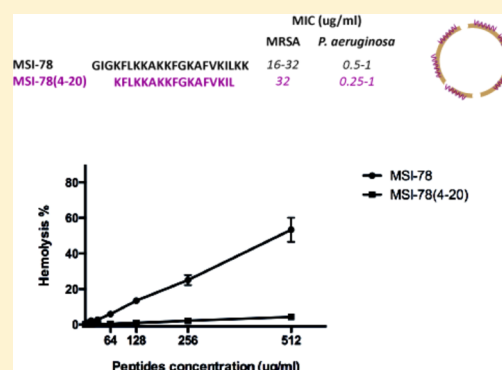
<sup>#</sup>ICBAS, Instituto de Ciências Biomédicas Abel Salazar, Universidade do Porto, Rua de Jorge Viterbo Ferreira 228, 4050-313 Porto, Portugal

<sup>¶</sup>IPATIMUP - Institute of Molecular Pathology and Immunology of the University of Porto, Rua Dr. Roberto Frias, 4200-465 Porto, Portugal

<sup>Δ</sup>IBMC-Instituto de Biologia Celular e Molecular, Unidade de Produção e Purificação de Proteínas, Universidade do Porto, Rua do Campo Alegre 823, 4150-180 Porto, Portugal

**ABSTRACT:** Antimicrobial peptides are widely recognized as an excellent alternative to conventional antibiotics. MSI-78, a highly effective and broad spectrum AMP, is one of the most promising AMPs for clinical application. In this study, we have designed shorter derivatives of MSI-78 with the aim of improving selectivity while maintaining antimicrobial activity. Shorter 17-mer derivatives were created by truncating MSI-78 at the N- and/or C-termini, while spanning MSI-78 sequence. Despite the truncations made, we found a 17-mer peptide, MSI-78(4–20) (KFLKKAKKFGKAFVKIL), which was demonstrated to be as effective as MSI-78 against the Gram-positive *Staphylococcus* strains tested and the Gram-negative *Pseudomonas aeruginosa*. This shorter derivative is more selective toward bacterial cells as it was less toxic to erythrocytes than MSI-78, representing an improved version of the lead peptide. Biophysical studies support a mechanism of action for MSI-78(4–20) based on the disruption of the bacterial membrane permeability barrier, which in turn leads to loss of membrane integrity and ultimately to cell death. These features point to a mechanism of action similar to the one described for the lead peptide MSI-78.

**KEYWORDS:** antimicrobial peptides, pexiganan, MSI-78, antibiotic resistance, cytotoxicity, membrane models



## INTRODUCTION

Antibiotic resistance is becoming a huge concern, with recent reports from the World Health Organization (WHO) showing worrying situations worldwide.<sup>1</sup> Methicillin resistant *Staphylococcus aureus* (MRSA) is one of the bacterial strains that cause most alarm, it was estimated that 25% of *S. aureus* isolates in the USA are resistant while this percentage can be even higher in other countries.<sup>2</sup> Resistance is also a problem in Gram-negative bacteria, such as in the case of multiresistant *Pseudomonas aeruginosa*, with statistics revealing that in some countries multiresistant *Pseudomonas* represent up to 45% of the isolates.<sup>3</sup>

The increasing emergency to combat resistant bacterial strains has prompted the development of new generations of antimicrobial agents, with antimicrobial peptides (AMP) being one of the most promising alternatives.<sup>4–7</sup>

AMP are ubiquitous in nature, usually 10–50 residues in length, and have the ability to interact with bacterial cell membranes most often leading to membrane disruption.<sup>8–10</sup> As their mode of action does not involve specific interactions, bacteria are less prone to acquire resistance to AMP.<sup>11</sup> However, some resistance mechanisms that involve alterations of the cell wall have been identified.<sup>11,12</sup>

Although AMP are promising antibiotic alternatives, their low stability and high toxicity prevent efficient therapeutic application.<sup>13</sup> Therefore, improving AMP potency and selectivity toward bacterial cells is needed. AMP selectivity is mainly

**Received:** February 5, 2015

**Revised:** June 2, 2015

**Accepted:** June 11, 2015

**Published:** June 11, 2015



determined by charge and hydrophobicity. While net charge is crucial in the establishment of electrostatic interactions between the positively charged peptide and the negatively charged lipid headgroup of the bacterial lipid bilayer, hydrophobicity is determinant in the insertion of the AMP into the lipid bilayer.<sup>14</sup>

Another concern for bringing AMP into therapeutic applications is the high cost of production associated with peptide synthesis. Therefore, developing short AMP with higher bacterial cell selectivity is the purpose of this study.<sup>13</sup> In fact, it has been reported that AMP length affects cytotoxicity, for example a 15 residue shortened melitin and a shorter derivative of HP(2–20) were 300 times less toxic to erythrocytes than their parent peptides.<sup>15–17</sup>

MSI-78 is a well-studied AMP, commercially known as pexiganan, developed for the treatment of infected diabetic foot ulcers.<sup>18,19</sup> This peptide has a broad spectrum of activity, being effective against Gram-positive and Gram-negative bacteria.<sup>18,20</sup> MSI-78 belongs to the class of  $\alpha$ -helical AMPs, and it has been described to form dimers stabilized by hydrophobic interactions.<sup>21</sup> Moreover, it is known that the MSI-78 mechanism of action involves disruption of bacterial membranes via toroidal-type pore formation.<sup>20</sup> Being one of the best-studied and efficient AMPs, MSI-78 is an excellent lead peptide to create shorter derivatives.

In this work, we aimed at creating a shorter MSI-78 derivative while maintaining antimicrobial activity. We identified a 17-mer peptide, MSI-78(4–20), which was demonstrated to be as effective as MSI-78 against all strains tested, despite the truncations made.

With the help of model biomembrane systems we unraveled the mechanism of action of MSI-78(4–20). Model membranes composed of different phospholipids that mimic bacterial and mammalian cell membrane were chosen as they are excellent models to characterize the interactions between membrane active compounds and bacterial or mammalian membranes. To mimic the mammalian membrane 1,2-dimyristoyl-*sn*-glycero-phosphocholine (DMPC) was chosen as it is widely used.<sup>22,23</sup> To mimic the bacterial membrane, a mixture of 1-palmitoyl-2-oleoyl-*sn*-glycero-3-phosphocholine (POPC) and 1-palmitoyl-2-oleoyl-*sn*-glycero-3-phosphoglycerol (POPG) at 1:1 molar ratio was chosen as it has been described as one of the most biologically relevant model membranes for studying the *S. aureus* strain.<sup>24</sup>

## ■ EXPERIMENTAL SECTION

**Reagents.**  $N^{\alpha}$ -Fmoc-protected amino acids, Rink amide AM resin, and 2-(1*H*-benzotriazole-1-yl)-1,1,3,3-tetramethyluronium hexafluorophosphate (HBTU) for solid phase peptide synthesis (SPPS) were from NovaBiochem-EMD4Biosciences (Darmstadt, Germany). *N*-Ethyl-*N,N*-diisopropylamine (DIEA), 1-hydroxybenzotriazole (HOBt), trifluoroacetic acid (TFA), triisopropylsilane (TIS), piperidine, and all solvents for SPPS were from Sigma-Aldrich (St. Louis, MO, USA). Octadecylsilane stationary phase 238TPB1520 for peptide purification by medium-pressure reverse-phase liquid chromatography (MP-RPLC) was from Vydac (Hesperia, CA, USA). The lipids, 1,2-dimyristoyl-*sn*-glycero-3-phosphocholine (DMPC), 1-palmitoyl-2-oleoyl-*sn*-glycero-3-phosphocholine (POPC), and 1-palmitoyl-2-oleoyl-*sn*-glycero-3-phosphoglycerol (POPG) with a purity grade >98% were also purchased from Sigma-Aldrich Co. Hepes buffer used in the biophysical experiments with LUVs consisted of 10 mmol L<sup>-1</sup> *N*-(2-hydroxyethyl)-piperazine-*N'*-(2-ethanesulfonic acid), and the ionic strength was

adjusted to 0.1 M with sodium chloride and the pH to 7.4. In the circular dichroism (CD) experiments, the buffer consisted of 10 mmol L<sup>-1</sup> sodium phosphate buffer, and the ionic strength was adjusted to 0.1 M with sodium fluoride and the pH to 7.4. Hepes and sodium phosphate buffer were supplied by Sigma-Aldrich Co. (St. Louis, MO, USA). All the other chemicals were purchased from Merck.

**Peptide Design and Synthesis.** Peptide sequences were designed in order to obtain 17-mer peptides based on MSI-78 sequence, while spanning the entire sequence with one 1 AA shifts with the aim of identifying shorter but still active fragments of MSI-78 (Table 1). The 17-mer length was chosen

**Table 1. Amino Acid Sequences of Synthetic Peptides Derived from MSI-78<sup>a</sup>**

peptides	amino acid sequence
MSI-78	GIGKFLKKAKKFGKAFVKILKK 22 AA
MSI-78(1–17)	GIGKFLKKAKKFGKAFV 17 AA
MSI-78(2–18)	IGKFLKKAKKFGKAFVK
MSI-78(3–19)	GKFLKKAKKFGKAFVKI
MSI-78(4–20)	KFLKKAKKFGKAFVKIL
MSI-78(5–21)	FLKKAKKFGKAFVKILK
MSI-78(6–22)	LKKAKKFGKAFVKILKK

<sup>a</sup>The 17-mer peptides were designed to span MSI-78 by 1-residue shift.

as it is an intermediate size between the 22-mer MSI-78 and the 12-mer short derivatives of MSI-78, that considerably lost its spectrum of activity as previously described by us.<sup>25</sup> Moreover, it has been shown that truncating peptides while maintaining a length above 15 AA may preserve antimicrobial activity.<sup>26</sup>

All peptides (Table 1) were prepared as C-terminal amides by standard Fmoc/<sup>t</sup>Bu SPPS on a Liberty1 microwave (MW) peptide synthesizer (CEM Corporation, Mathews, NC, USA).<sup>27</sup> Briefly, Rink amide AM resin was preswelled for 15 min in *N,N*-dimethylformamide (DMF) and then transferred into the MW-reaction vessel. The initial Fmoc deprotection step was carried out using 20% piperidine in DMF containing 0.1 M HOBt in two MW irradiation pulses: 30 s at 24 W plus 3 min at 28 W, in both cases temperature being kept under 75 °C. The Fmoc-protected C-terminal amino acid (Bachem, Switzerland) was then coupled to the resin, using 5 molar equiv of the Fmoc-protected amino acid in DMF (0.2 M), 5 equiv of 0.5 M HBTU/HOBt in DMF, and 10 equiv of 2 M DIEA in *N*-methylpyrrolidone (NMP); the coupling step was carried out for 5 min at 35 W MW irradiation, with maximum temperature kept below 75 °C. The remaining amino acids were sequentially coupled in the C → N direction by means of similar deprotection and coupling cycles. Following completion of sequence assembly, the peptides were released from the resin with concomitant removal of side-chain protecting groups, by a 3 h acidolysis at room temperature using a TFA-based cocktail containing TIS and water as scavengers (TFA/TIS/H<sub>2</sub>O 95:2.5:2.5 v/v/v). Crude products were purified by MP-RPLC to a purity of at least 95%, as confirmed by high-performance liquid chromatography (HPLC) analysis on a Hitachi-Merck LaChrom Elite system equipped with a quaternary pump, a thermostated (Peltier effect) automated sampler, and a diode-array detector (DAD). Pure peptides were quantified by UV-absorption spectroscopy (Helios Gama, Spectronic Unicam) and their molecular weights confirmed to be as expected by electrospray ionization/ion trap mass

spectroscopy (ESI/IT MS; LCQ-DecaXP LC–MS system, ThermoFinnigan).

**Microorganisms and Growth Conditions.** Microorganisms tested in this study were the following: *Staphylococcus aureus* (*S. aureus*) ATCC 33591 (methicillin resistant), *S. aureus* ATCC 25932, *Staphylococcus epidermidis* ATCC 35984, and *P. aeruginosa* ATCC 27853. Bacteria were grown on trypticase soy agar (TSA) plates and Mueller–Hinton broth (MHB).

**Antimicrobial Testing.** Antimicrobial activity was assessed by minimum inhibitory concentration (MIC) and minimum bactericidal concentration (MBC). The method used to determine the MIC was the broth microdilution assay in microtiter plates, described by Wiegand and co-workers.<sup>28</sup> This method follows the guidelines of the two recognized organizations, CLSI and EUCAST. Bacteria were precultured on TSB overnight at 37 °C and 150 rpm. After washing with phosphate buffered saline (PBS), bacteria were adjusted to approximately  $2 \times 10^5$  CFU/mL in MHB, and 99  $\mu$ L was transferred to a 96 well plate. Polypropylene microtiter plates were used to prevent binding of the peptides to the walls of the wells. Peptide dilutions were prepared in acetic acid/bovine serum albumin (BSA) solution, and peptide concentrations tested ranged from 512  $\mu$ g/mL to 0.015  $\mu$ g/mL, adjusted according to results obtained in preliminary experiments. The peptides were tested in a final volume of 110  $\mu$ L.

The minimum bactericidal concentration (MBC) was determined by plating the content of the first three wells where visible growth was not observed.

**Hemolysis Assay on Human Red Blood Cells (RBC).** Human blood buffy coats were obtained from healthy volunteers (Centro Hospitalar de São João, EPE, Porto, Portugal) and processed to obtain RBC by centrifugation over density gradient with Histopaque-1077, Sigma-Aldrich Co. (St. Louis, MO, USA) according to the manufacturer's instructions. After removal of the plasma upper layer, the lower layer containing RBC was washed three times in PBS. The purified RBC were diluted to  $(6-7) \times 10^8$  cells/mL in PBS, and 99  $\mu$ L was distributed in a 96 well polypropylene microtiter plate.

Peptide dilutions were prepared in acetic acid/BSA solution, and the range of peptide concentrations tested went from 512  $\mu$ g/mL to 1  $\mu$ g/mL. After 1 h of incubation at 37 °C under 5% CO<sub>2</sub>, cells were centrifuged at 900 g for 10 min, and the supernatant was transferred to a 96 well plate. The absorbance values of the released hemoglobin were determined at 450 nm using a microplate reader (SynergyMx, Biotek). Untreated cells were used as negative control and cells treated with 0.2% Triton X-100 as positive controls. The percentage hemolysis was calculated as  $[(\text{sample absorbance} - \text{negative control absorbance})/(\text{positive control absorbance} - \text{negative control absorbance})] \times 100$ .

**Preparation of Cell Membrane Models: Large Unilamellar Vesicles (LUVs).** Lipid films were formed from chloroform solution of DMPC and POPC:POPG 1:1 molar ratio lipids, dried under a stream of nitrogen and left under reduced pressure for a minimum of 45 min, to remove all traces of the organic solvent. LUVs were prepared by the addition of the buffer, followed by vortexing, yielding multilamellar vesicles (MLVs). Lipid suspensions were equilibrated at  $37.0 \pm 0.1$  °C for 30 min and extruded 10 times through polycarbonate filters with a diameter pore of 100 nm to form LUVs, as previously described.<sup>23</sup>

**$\zeta$ -Potential of LUVs.** The  $\zeta$ -potential of LUVs in the absence and in the presence of AMP was assessed through the

determination of the electrophoretic mobility using a ZetaPALS (Brookhaven Instruments Corporation). Typically 10 runs were performed and the temperature was maintained at  $37.0 \pm 0.1$  °C, the lipid concentration being kept constant at 200  $\mu$ M, and AMP concentration ranged from 0–40  $\mu$ M.

**Hydrodynamic Diameter.** The hydrodynamic diameters of LUVs in the absence and in the presence of AMP were determined in a BI-MAS dynamic light scattering (DLS) instrument (Brookhaven Instruments, USA). Typically 6 runs (2 min each) were performed at the temperature of  $37.0 \pm 0.1$  °C, the cumulate analysis being applied to scattering data to give effective diameters and polydispersity.

**Circular Dichroism (CD) Analysis.** The secondary structure of the peptides MSI-78(4–20) and MSI-78 was investigated using CD on a JASCO J-815 spectropolarimeter, equipped with a temperature-controlled cuvette and controlled by the Spectra manager software.

Peptide solutions were diluted in 10 mM sodium phosphate, pH 7.4, 100 mM sodium fluoride to a concentration of 40  $\mu$ M with and without 5 mM DMPC or POPC:POPG 1:1 molar ratio LUVs, corresponding to a peptide:lipid molar ratio of 1:125.

Before the measurement all peptide solutions were incubated at 37 °C for 30 min. Far-UV CD spectra were recorded between 195 and 260 nm using a 1 mm path length cuvette. CD spectra were acquired with a scanning speed of 100 nm/min and an integration time of 1 s, and using a bandwidth of 1 nm. The spectra were averaged over 16 scans and corrected by subtraction of the buffer or buffer plus LUVs signal.

The results are expressed as the mean residue ellipticity  $\theta_{MRW}$ , defined as  $\theta_{MRW} = \theta_{obs}(0.1 MRW)/(lc)$ , where  $\theta_{obs}$  is the observed ellipticity in millidegrees, MRW is the mean residue weight,  $c$  is the concentration in mg/mL, and  $l$  is the light path length in centimeters.

The mean helix content ( $f_H$ ) was calculated according to Luo and Baldwin, 1997.<sup>29</sup> Briefly,  $f_H$  is obtained from the  $\theta_{MRW}$  at 222 nm of each peptide ( $\theta_{222}$ ) according to the equation  $f_H = (\theta_{222} - \theta_C)/(\theta_H - \theta_C)$ , where the baseline ellipticities for random coil ( $\theta_C$ ) and complete helix ( $\theta_H$ ) are given by  $\theta_C = 2220 - 53T$  and  $\theta_H = (-44000 + 250T)(1 - 3/N)$ , where  $T$  is the temperature in °C and  $N$  is the chain length in number of residues.

## RESULTS

**Antimicrobial Activity.** MIC of MSI-78 and its 17-mer derivatives against the Gram-positive *S. aureus* and *S. epidermidis* and the Gram-negative *P. aeruginosa* are described in Table 2.

Regarding Gram-positive *S. aureus* strains, the 17-mer peptide MSI-78(4–20) was the most effective with MIC values of 32  $\mu$ g/mL for the MRSA strain and 8–16  $\mu$ g/mL for the nonresistant *S. aureus* strain. Similar MIC values were obtained with the lead peptide (MSI-78). MSI-78(1–17) maintained also a high antimicrobial activity with MIC values of 64–128  $\mu$ g/mL for the MRSA strain and 32  $\mu$ g/mL for the nonresistant *S. aureus* strain. The MRSA strain is slightly less susceptible to the peptides than the nonresistant strain. *S. epidermidis* ATCC 35984 was more susceptible to the MSI-78 derivatives than *S. aureus* with all the 17-mer peptides being effective with MIC values ranging from 2 to 32  $\mu$ g/mL. Still, MSI-78(4–20) also proved to be the most effective 17-mer derivative against this strain. Results for the Gram-negative *P. aeruginosa* demonstrate that this strain is much more



Table 2. Determination of MIC and MBC of MSI-78 and 17-mer Derivatives against Selected Microorganisms<sup>a</sup>

peptides	microorganisms							
	<i>S. aureus</i> (MRSA)		<i>S. aureus</i>		<i>S. epidermidis</i>		<i>P. aeruginosa</i>	
	MIC	MBC	MIC	MBC	MIC	MBC	MIC	MBC
MSI-78	16–32 (6.5–13)	32	8–16 (3.2–6.5)	8–16	0.5–1 (0.2–0.4)	0.5–1	0.5–1 (0.2–0.4)	1–4
MSI-78(1–17)	64–128	256	32	32–64	4–8	8–16	0.5–2	2–4
MSI-78(2–18)	>512		>512		16–32	32–64	4–8	>16
MSI-78(3–19)	512	>512	256	256–512	8–16	16–32	1–2	2–4
MSI-78(4–20)	32 (16)	64	8–16 (4–8)	16–32	2 (1)	2–4	0.25–1 (0.1–0.5)	1–4
MSI-78(5–21)	256	256–512	64–128	128–256	2–4	4	1–4	4–8
MSI-78(6–22)	>512		>512		8–32	16–64	2–4	2–8

<sup>a</sup>MIC values are presented in  $\mu\text{g/mL}$ . Concentrations in  $\mu\text{M}$  are in parentheses.

susceptible to the 17-mer peptides and to MSI-78 than Gram-positive *Staphylococcus* strains. All 17-mer peptides maintained the antibacterial effect with MIC values below 8  $\mu\text{g/mL}$ , the MIC for MSI-78 being exceptionally low, 0.5–1  $\mu\text{g/mL}$ . MSI-78(4–20) was the most effective of all 17-mer derivatives also against *P. aeruginosa*.

Overall, we found two 17-mer peptides, MSI-78(4–20) and MSI-78(1–17), that maintained high spectrum of activity, being effective against all strains tested, with MSI-78(4–20) standing out, as it demonstrated to be equipotent to MSI-78.

MBC results were in general within the same range or 2-fold higher than MIC results, indicating bactericidal effect of the peptides for the concentrations tested.

MSI-78 antimicrobial activity was in general found to be in line with previously published studies. Although MSI-78 MIC values obtained for *S. epidermidis* and *P. aeruginosa* are slightly lower than published data, some variation is reported in the literature for these strains.<sup>18,20,30</sup>

**Hemolytic Activity.** Cytotoxicity studies were performed with MSI-78 and MSI-78(4–20), as it demonstrated to be as effective as the lead peptide.

MSI-78(4–20) was less cytotoxic to RBC than the lead AMP, MSI-78 (Figure 1). MSI-78 showed some toxicity at high

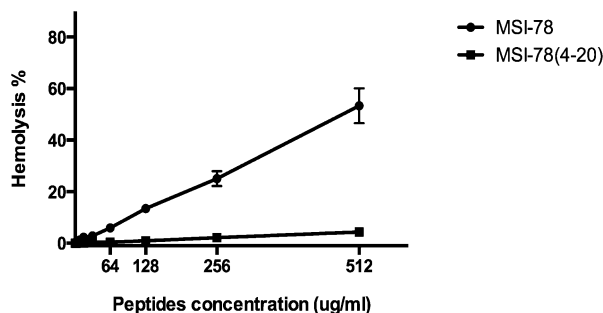


**Figure 1.** Hemolytic activity of MSI-78 and MSI-78(4–20) on human RBC. Peptide concentrations tested covered a range from 512  $\mu\text{g/mL}$  to 1  $\mu\text{g/mL}$ . Untreated bacterial cells were used as negative control, and bacterial cells treated with 0.2% Triton X-100 were used as positive control.

concentrations (53% hemolysis at 512  $\mu\text{g/mL}$ , 25% hemolysis at 256  $\mu\text{g/mL}$ , and 13% hemolysis at 128  $\mu\text{g/mL}$ ), which is in agreement with previously published data.<sup>31</sup> The 17-mer peptide, MSI-78(4–20), showed very low toxicity to RBC even at the higher concentrations tested (4% hemolysis at 512  $\mu\text{g/mL}$ , 2% hemolysis at 256  $\mu\text{g/mL}$ , and 1% hemolysis at 128  $\mu\text{g/mL}$ ).

### AMP Interaction with Membrane Mimetic Systems.

**$\zeta$ -Potential.** The  $\zeta$ -potential of DMPC and POPC:POPG LUVs in the absence and in the presence of the AMPs MSI-78(4–20) and MSI-78 is represented in Figure 2. The determined  $\zeta$ -potential of the zwitterionic DMPC LUVs was as expected close to zero.<sup>32</sup> In the presence of MSI-78(4–20) or MSI-78, the  $\zeta$ -potential remains nearly unchanged (Figure 2A). The addition of increased concentrations of either peptide to DMPC LUVs caused almost no alteration on the zeta potential values, suggesting a weak interaction or non-interaction with the mammalian membrane model. The  $\zeta$ -potential of POPC:POPG LUVs was as expected negative, being significantly altered by addition of either AMP and becoming less negative as the concentration of MSI-78(4–20) and MSI-78 increased (Figure 2B).<sup>33</sup> An overall change from approximately  $-28$  mV to nearly neutral potential values was achieved after the addition of both peptides (Figure 2B). However, the variation of the  $\zeta$ -potential values was even more evident in the case of MSI-78 for lower concentrations (below 20  $\mu\text{M}$ ) of peptide (Figure 2B). These results suggest that the positively charged peptides interact with the negatively charged POPC:POPG LUVs, inducing changes in the membrane surface charge by direct peptide binding and/or insertion in the bacterial membrane model. The MSI-78 more pronounced effect is probably due to the high positive charge displayed (+9) in comparison to MSI-78(4–20) (+7), being consequently more prone to establish electrostatic interactions with the negatively charged bacterial membrane.

**Hydrodynamic Diameter.** The size of DMPC and POPC:POPG LUVs in the absence and presence of different concentrations of the AMPs MSI-78(4–20) and MSI-78 is represented in Figure 3. In the absence of peptides, DMPC and POPC:POPG LUVs presented a size of approximately 100 nm (Figure 3A), as expected regarding their preparation. In the presence of the peptides, DMPC LUVs exhibited a narrow size distribution with a mean diameter of approximately 103–118 nm (Figure 3A), pointing to a weak influence or noninfluence of both peptides in the mammalian cell membrane model even at high peptide concentrations. On the other hand, peptide interactions with POPC:POPG LUVs induced a pronounced increase of the LUVs size, at peptide concentrations higher than 10  $\mu\text{M}$  (Figure 3B). Moreover, this result is emphasized by the high polydispersity values obtained, indicating the presence of a heterogeneous population (polydispersity >0.1) (Figure 3B), and pointing to the existence of aggregated structures. Therefore, bacterial membrane model binding facilitates nucleation-dependent AMP aggregation. The aggregation explains the larger mean hydrodynamic diameter

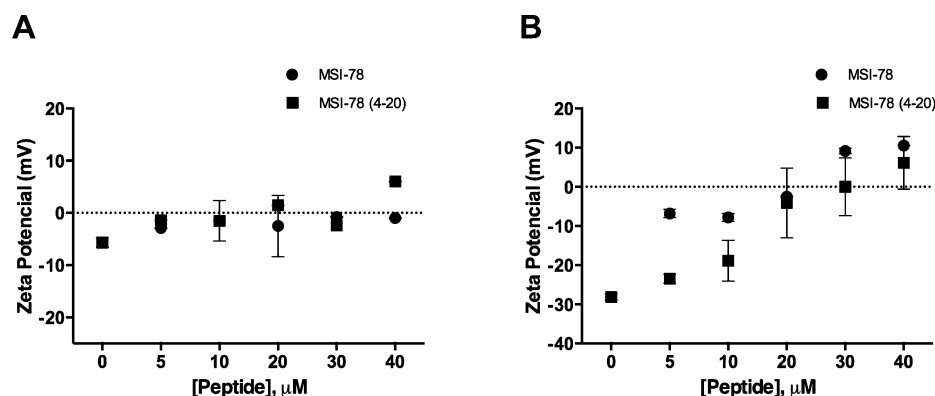


**Figure 2.** Zeta potential measurements of 200  $\mu\text{M}$  DMPC (A) and POPC:POPG molar ratio 1:1 mixture (B) after 30 min incubation and stabilization with MSI-78(4–20) and MSI-78 at 37  $^{\circ}\text{C}$ . Circles MSI-78, squares MSI-78(4–20). Error bars represent the standard deviation of at least three independent experiments.

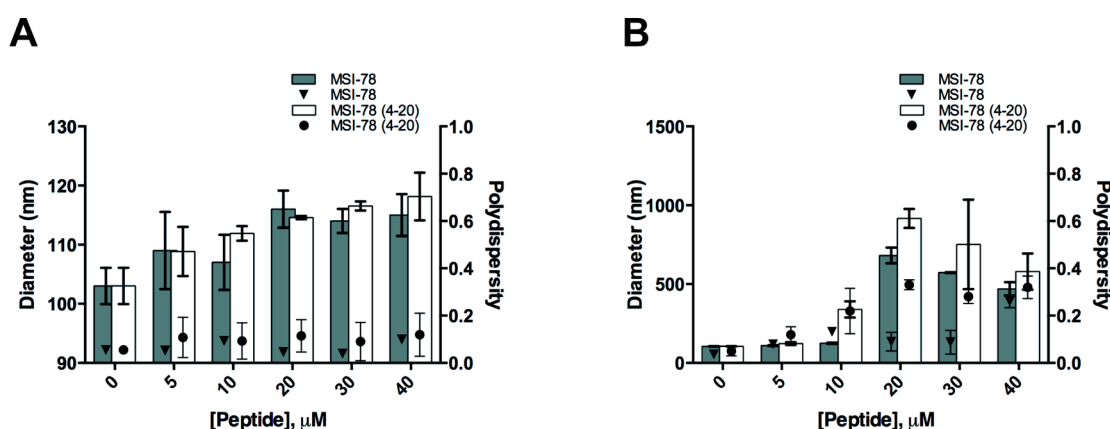


**Figure 3.** Hydrodynamic diameters of 200  $\mu\text{M}$  DMPC (A) and POPC:POPG 1:1 molar ratio mixture (B) after 30 min incubation and stabilization with MSI-78 and MSI-78(4–20) at 37  $^{\circ}\text{C}$ . Bars represent diameters (nm), and dots represent polydispersity. Error bars represent the standard deviation of at least three independent experiments.

and polydispersity obtained in the case of POPC:POPG LUVs for higher AMP concentrations.

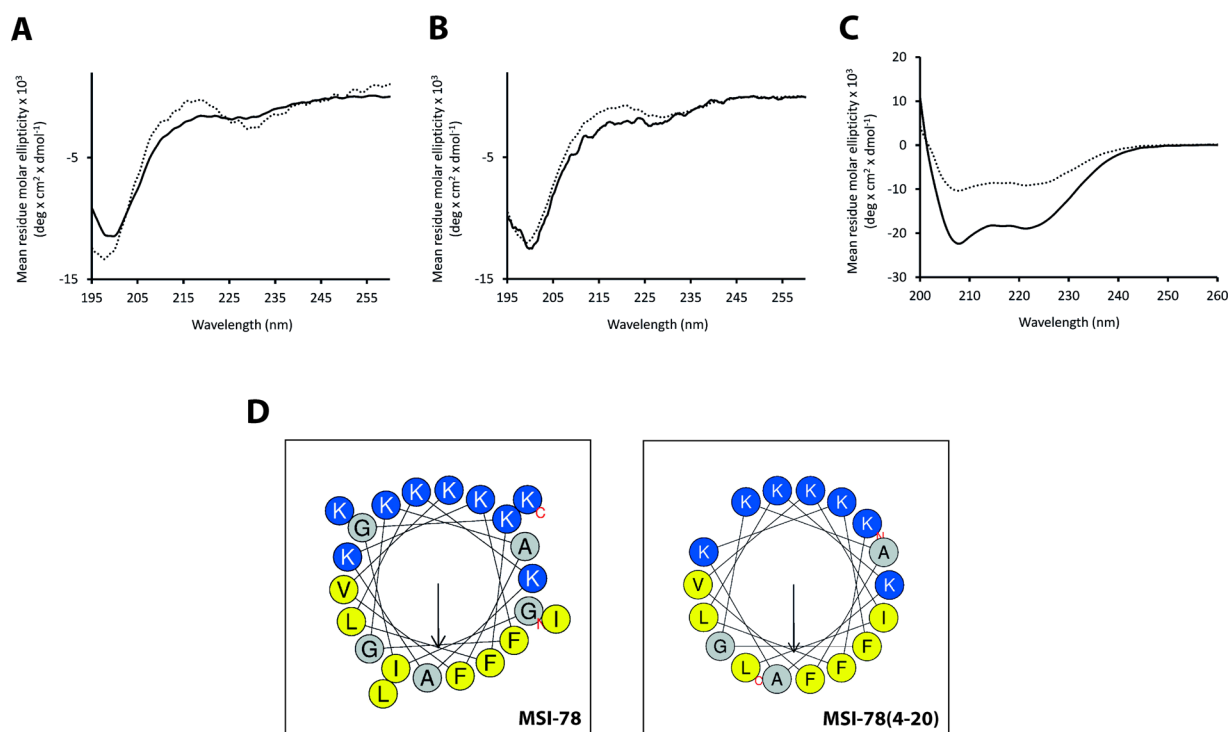
**AMP Structural Analysis (Secondary Structure).** CD spectra of MSI-78 and MSI-78(4–20) in aqueous buffer exhibited a negative minimum at  $\approx 198$  nm suggesting random coil conformations (Figure 4A). In the presence of DMPC LUVs, spectra also exhibit characteristic profiles of unordered peptides, pointing out to no toxicity toward mammalian cells (Figure 4B). In the presence of POPC:POPG (1:1 molar ratio) LUVs, two negative minima at  $\approx 208$  nm and  $\approx 222$  suggest the presence of  $\alpha$ -helical conformations (Figure 4C). For all peptides, results indicate a transition from a random coil to an ordered secondary structure upon interaction with the bacterial membrane mimetic system POPC:POPG LUVs. In the presence of this system, calculated mean helix contents show slight differences between the peptides. The lead 22-mer peptide MSI-78 has 62% helicity, whereas helicity values around 40–45% have been reported by Mercke et al. for this peptide when bound to POPC small unilamellar vesicles (SUV).<sup>34,35</sup> For MSI-78(4–20) the determined mean helix content was 33%, which shows a difference of approximately 30% in the helix content between the two peptides.

Figure 4D represents the helical wheel projections of the peptides where the relative position of the amino acids and its polar/nonpolar character is displayed. Table 3 summarizes the physicochemical properties and structural analysis of the

peptides. MSI-78(4–20) displays higher hydrophobicity and higher hydrophobic moment than MSI-78. However, no hydrophobic face is predicted for MSI-78(4–20) by Heliquest, as it is not presenting a face of at least five uninterrupted hydrophobic residues in the  $\alpha$ -helix.<sup>36</sup>

## DISCUSSION

In this study, we aimed at finding a short 17-mer fragment of MSI-78, while maintaining MSI-78 antimicrobial activity. We found two 17-mer fragments that maintained a high spectrum of activity, MSI-78(1–17) and MSI-78(4–20). As MSI-78(4–20) was as effective as MSI-78 against all strains tested, we chose this peptide to study in more detail. Several physicochemical parameters have been associated with a good AMP performance, among them: size, sequence, charge, secondary structure, hydrophobicity, and amphipathicity. Although MSI-78(4–20) is shorter and possesses a net charge lower than MSI-78, hydrophobicity and amphipathicity parameters favor MSI-78(4–20) antimicrobial activity. On the other hand, while MSI-78(4–20) structures as an  $\alpha$ -helix, the percentage of helicity is about half when compared to MSI-78, however, this does not seem to be determinant for antimicrobial activity. It has been shown that AMP secondary structure and biological activity are not always coupled.<sup>37,38</sup> The absence of a glycine in the N-terminus of MSI-78(4–20) might contribute to the smaller  $\alpha$ -helical content in comparison to MSI-78 as the glycine



**Figure 4.** CD spectra of peptides MSI-78 (solid line) and MSI-78(4–20) (dotted line) acquired in aqueous buffer (A) and in the presence of DMPC (B) and POPC/POPG (C) LUVs. Heliquet helical wheel projection diagrams of MSI-78 and MSI-78(4–20) (D); apolar residues are represented in yellow and polar residues in blue.

**Table 3. Physicochemical Properties and Structural Analysis of MSI-78 and MSI-78(4–20)<sup>a</sup>**

peptides	mol wt	charge	<i>H</i>	$\mu$ H	aliphatic index	predicted hydrophobic face <sup>b</sup>	helicity (% helix)
MSI-78	2476	+9	0.241	0.674	93.18	FFFAILGLV	62%
MSI-78(4–20)	1995	+7	0.322	0.704	97.65	none	33%

<sup>a</sup>The values for net charge (*z*), hydrophobicity (*H*), and mean hydrophobic moment ( $\mu$ H) were assessed using the analysis module of Heliquet.<sup>36</sup> Aliphatic index was obtained using The Collection of Anti-Microbial Peptides (CAMP). <sup>b</sup>Hydrophobic face predicted by Heliquet; this algorithm detects the existence of an uninterrupted hydrophobic face of at least 5 residues adjacent on a helical wheel.

N-capping stabilizing effect is well-known.<sup>39</sup> The biophysical studies show that both peptides interact preferentially with the bacterial cell membrane model, the membrane disruption being concentration-dependent.<sup>40</sup> The proposed interaction of both peptides with the bacterial membrane initiates with peptide binding to the membrane surface through electrostatic interactions, which is especially pronounced in the case of MSI-78. In the case of MSI-78(4–20), its higher hydrophobicity (higher *H* and  $\mu$ H) can favor a deeper insertion within the bacterial lipid bilayer, which may explain its ability to exert a bacterial effect despite its lower ability to form  $\alpha$ -helices.<sup>41</sup> These results are in line with the published MSI-78 mechanism of interaction with bacterial membrane models, involving induction of substantial changes in lipid bilayers via positive curvature strain and toroidal pore formation.<sup>42</sup>

We have also found that MSI-78(4–20) is less hemolytic than MSI-78, which represents a major advantage of the 17-mer AMP as compared to the lead MSI-78. In fact, as MSI-78(4–20) displays a lower net charge than MSI-78 (+7 and +9 respectively), this can be determinant for the initial interaction between the peptide and the mammalian membrane. While hydrophobicity parameter values would point to a higher hemolytic activity of MSI-78(4–20), this did not occur. It has been reported that increase of *H* and  $\mu$ H substantially enhance hemolytic activity, however, MSI-78(4–20) does not possess a

well-defined hydrophobic face, as predicted by Heliquet. For MSI-78, such a hydrophobic face is predicted, which may maximize the hydrophobic interactions of the nonpolar face of the amphipathic helix and the lipid, in the case of  $\alpha$ -helix formation upon interaction with RBC.<sup>36,43–45</sup> In fact, disruption of the hydrophobic face with a lysine substitution in the nonpolar sector of a helical wheel projection has been observed to improve peptide selectivity, while reduction of helical content has been associated with decreased hemolytic activity.<sup>46,47</sup>

Therefore, the more pronounced hemolytic effect of MSI-78 may be attributed to the marked nonspecific hydrophobic interactions between the peptide and the mammalian cell membranes.

The perturbation of the lipid bilayers by a peptide is indeed governed by a balance between electrostatic and hydrophobic interactions. Our results clearly indicate the importance of the balance of these forces, suggesting this effect to be highly responsible for the MSI-78(4–20) improved selectivity toward bacterial cells and the ability to overcome the hemolytic toxic effects of MSI-78. Still, differences between the peptides regarding interactions with the mammalian membrane model DMPC LUVs were not observed, however a membrane model does not mimic a mammalian cell with its inherent complexity. In fact to obtain the full picture of the peptides' mechanism of



action, more detailed studies will need to be carried out, including the use of more complex membrane models with other compounds present in biological membranes (e.g., cholesterol, phosphatidylethanolamines, proteins), and also intact cells.<sup>48</sup> Nevertheless, the biophysical properties reported in this study will be useful in designing membrane specific antimicrobial peptides.

In this study, we found a very effective and broad-spectrum AMP, MSI-78(4–20). This MSI-78 derivative is as effective as the lead peptide, while having reduced hemolytic activity, thus representing an improved version of MSI-78. We can envisage a wide application for this AMP in the field of antimicrobial research and possibly in the field of anticancer therapy, as a number of other synthetic magainin analogues demonstrated promising anticancer activity.<sup>49</sup>

## AUTHOR INFORMATION

### Corresponding Author

\*INEB—Instituto de Engenharia Biomédica, Rua do Campo Alegre 823, 4150-180 Porto, Portugal. Tel: +351 22 6074982. Fax: +351 22 6094567. E-mail: cmartins@ineb.up.pt.

### Notes

The authors declare no competing financial interest.

<sup>§</sup>C.M. and M.P. contributed equally.

## ACKNOWLEDGMENTS

This work was financed by FEDER funds through the Programa Operacional Factores de Competitividade (COMPETE) and by Portuguese funds through FCT (Fundação para a Ciência e a Tecnologia) in the framework of the Projects PTDC/CTM/101484/2008, PEst-C/SAU/LA0002/2013, Portugal-China joint Innovation Centre for Advanced Materials (JICAM2013), and the following grants: SFRH/BPD/79439/2011 (C.M.), SFRH/BPD/99124/2013 (M.P.), and SFRH/BD/89001/2012 (C.L.S.). The authors also thank FCT for supporting research unit UCIBIO-REQUIMTE through project UID/Multi/04378/2013. The authors would like to thank Centro Hospitalar de São João, EPE, Porto, for the human buffy coats.

## ABBREVIATIONS USED

AMP, antimicrobial peptide; MIC, minimum inhibitory concentration; MBC, minimum bactericidal concentration

## REFERENCES

- (1) WHO. *Antimicrobial Resistance: Global Report on Surveillance 2014*; World Health Organization: April 2014.
- (2) Chambers, H. F.; Deleo, F. R. Waves of resistance: *Staphylococcus aureus* in the antibiotic era. *Nat. Rev. Microbiol.* **2009**, *7* (9), 629–41.
- (3) Avner, B. S.; Fialho, A. M.; Chakrabarty, A. M. Overcoming drug resistance in multi-drug resistant cancers and microorganisms: a conceptual framework. *Bioengineered* **2012**, *3* (5), 262–70.
- (4) Ziemska, J.; Rajnisz, A.; Solecka, J. New perspectives on antibacterial drug research. *Cent. Eur. J. Biol.* **2013**, *8* (10), 943–957.
- (5) Andres, E.; Dimarçq, J. L. Cationic antimicrobial peptides: update of clinical development. *J. Int. Med.* **2004**, *255* (4), 519–20.
- (6) Cruz, J.; Ortiz, C.; Guzman, F.; Fernandez-Lafuente, R.; Torres, R. Antimicrobial Peptides: Promising Compounds Against Pathogenic Microorganisms. *Curr. Med. Chem.* **2014**, *21* (20), 2299–321.
- (7) Fitzgerald-Hughes, D.; Devocelle, M.; Humphreys, H. Beyond conventional antibiotics for the future treatment of methicillin-resistant *Staphylococcus aureus* infections: two novel alternatives. *FEMS Immunol. Med. Microbiol.* **2012**, *65* (3), 399–412.
- (8) Brogden, K. A. Antimicrobial peptides: pore formers or metabolic inhibitors in bacteria? *Nat. Rev. Microbiol.* **2005**, *3* (3), 238–50.
- (9) Powers, J. P.; Hancock, R. E. The relationship between peptide structure and antibacterial activity. *Peptides* **2003**, *24* (11), 1681–91.
- (10) Epan, R. M.; Vogel, H. J. Diversity of antimicrobial peptides and their mechanisms of action. *Biochim. Biophys. Acta* **1999**, *1462* (1–2), 11–28.
- (11) Yeaman, M. R.; Yount, N. Y. Mechanisms of antimicrobial peptide action and resistance. *Pharmacol. Rev.* **2003**, *55* (1), 27–55.
- (12) Marr, A. K.; Gooderham, W. J.; Hancock, R. E. Antibacterial peptides for therapeutic use: obstacles and realistic outlook. *Curr. Opin. Pharmacol.* **2006**, *6* (5), 468–72.
- (13) Hancock, R. E.; Sahl, H. G. Antimicrobial and host-defense peptides as new anti-infective therapeutic strategies. *Nat. Biotechnol.* **2006**, *24* (12), 1551–7.
- (14) Matsuzaki, K. Control of cell selectivity of antimicrobial peptides. *Biochim. Biophys. Acta* **2009**, *1788* (8), 1687–92.
- (15) Bahar, A. A.; Ren, D. Antimicrobial peptides. *Pharmaceutics* **2013**, *6* (12), 1543–75.
- (16) Subbalakshmi, C.; Nagaraj, R.; Sitaram, N. Biological activities of C-terminal 15-residue synthetic fragment of melittin: design of an analog with improved antibacterial activity. *FEBS Lett.* **1999**, *448* (1), 62–6.
- (17) Park, Y.; Park, S. C.; Park, H. K.; Shin, S. Y.; Kim, Y.; Hahm, K. S. Structure-activity relationship of HP (2–20) analog peptide: enhanced antimicrobial activity by N-terminal random coil region deletion. *Biopolymers* **2007**, *88* (2), 199–207.
- (18) Ge, Y.; MacDonald, D. L.; Holroyd, K. J.; Thornsberry, C.; Wexler, H.; Zasloff, M. In vitro antibacterial properties of pexiganan, an analog of magainin. *Antimicrob. Agents Chemother.* **1999**, *43* (4), 782–8.
- (19) Lipsky, B. A.; Holroyd, K. J.; Zasloff, M. Topical versus systemic antimicrobial therapy for treating mildly infected diabetic foot ulcers: a randomized, controlled, double-blinded, multicenter trial of pexiganan cream. *Clin. Infect. Dis.* **2008**, *47* (12), 1537–45.
- (20) Gottler, L. M.; Ramamoorthy, A. Structure, membrane orientation, mechanism, and function of pexiganan—a highly potent antimicrobial peptide designed from magainin. *Biochim. Biophys. Acta* **2009**, *1788* (8), 1680–6.
- (21) Porcelli, F.; Buck-Koehntop, B. A.; Thennarasu, S.; Ramamoorthy, A.; Veglia, G. Structures of the dimeric and monomeric variants of magainin antimicrobial peptides (MSI-78 and MSI-594) in micelles and bilayers, determined by NMR spectroscopy. *Biochemistry* **2006**, *45* (18), 5793–9.
- (22) Ilic, N.; Novkovic, M.; Guida, F.; Xhindoli, D.; Benincasa, M.; Tossi, A.; Juretic, D. Selective antimicrobial activity and mode of action of adepantins, glycine-rich peptide antibiotics based on anuran antimicrobial peptide sequences. *Biochim. Biophys. Acta* **2013**, *1828* (3), 1004–12.
- (23) Pinheiro, M.; Arede, M.; Nunes, C.; Caio, J. M.; Moiteiro, C.; Lucio, M.; Reis, S. Differential interactions of rifabutin with human and bacterial membranes: implication for its therapeutic and toxic effects. *J. Med. Chem.* **2013**, *56* (2), 417–26.
- (24) Cheng, J. T.; Hale, J. D.; Elliott, M.; Hancock, R. E.; Straus, S. K. The importance of bacterial membrane composition in the structure and function of aurein 2.2 and selected variants. *Biochim. Biophys. Acta* **2011**, *1808* (3), 622–33.
- (25) Monteiro, C.; Fernandes, M.; Pinheiro, M.; Maia, S.; Seabra, C. L.; Ferreira-da-Silva, F.; Costa, F.; Reis, S.; Gomes, P.; Martins, M. C. Antimicrobial properties of membrane-active dodecapeptides derived from MSI-78. *Biochim. Biophys. Acta* **2015**, *1848* (5), 1139–46.
- (26) Deslouches, B.; Phadke, S. M.; Lazarevic, V.; Cascio, M.; Islam, K.; Montelaro, R. C.; Mietzner, T. A. De novo generation of cationic antimicrobial peptides: influence of length and tryptophan substitution on antimicrobial activity. *Antimicrob. Agents Chemother.* **2005**, *49* (1), 316–22.
- (27) Brandt, M.; Gammeltoft, S.; Jensen, K. Microwave Heating for Solid-Phase Peptide Synthesis: General Evaluation and Application to 15-mer Phosphopeptides. *Int. J. Pept. Res. Ther.* **2006**, *12* (4), 349–57.

- (28) Wiegand, I.; Hilpert, K.; Hancock, R. E. Agar and broth dilution methods to determine the minimal inhibitory concentration (MIC) of antimicrobial substances. *Nat. Protoc.* **2008**, 3 (2), 163–75.
- (29) Luo, P.; Baldwin, R. L. Mechanism of helix induction by trifluoroethanol: a framework for extrapolating the helix-forming properties of peptides from trifluoroethanol/water mixtures back to water. *Biochemistry* **1997**, 36 (27), 8413–21.
- (30) Chongsiriwatana, N. P.; Miller, T. M.; Wetzler, M.; Vakulenko, S.; Karlsson, A. J.; Palecek, S. P.; Mobashery, S.; Barron, A. E. Short alkylated peptoid mimics of antimicrobial lipopeptides. *Antimicrob. Agents Chemother.* **2011**, 55 (1), 417–20.
- (31) Zhang, Y.; Zhao, H.; Yu, G. Y.; Liu, X. D.; Shen, J. H.; Lee, W. H. Structure-function relationship of king cobra cathelicidin. *Peptides* **2010**, 31 (8), 1488–93.
- (32) Aleandri, S.; Bombelli, C.; Bonicelli, M. G.; Bordini, F.; Giansanti, L.; Mancini, G.; Ierino, M.; Sennato, S. Fusion of gemini based cationic liposomes with cell membrane models: implications for their biological activity. *Biochim. Biophys. Acta* **2013**, 1828 (2), 382–90.
- (33) Tunuguntla, R.; Bangar, M.; Kim, K.; Stroeve, P.; Ajo-Franklin, C. M.; Noy, A. Lipid bilayer composition can influence the orientation of proteorhodopsin in artificial membranes. *Biophys. J.* **2013**, 105 (6), 1388–96.
- (34) Mecke, A.; Lee, D. K.; Ramamoorthy, A.; Orr, B. G.; Banaszak Holl, M. M. Membrane thinning due to antimicrobial peptide binding: an atomic force microscopy study of MSI-78 in lipid bilayers. *Biophys. J.* **2005**, 89 (6), 4043–50.
- (35) Ramamoorthy, A.; Thennarasu, S.; Lee, D. K.; Tan, A.; Maloy, L. Solid-state NMR investigation of the membrane-disrupting mechanism of antimicrobial peptides MSI-78 and MSI-594 derived from magainin 2 and melittin. *Biophys. J.* **2006**, 91 (1), 206–16.
- (36) Gautier, R.; Douguet, D.; Antonny, B.; Drin, G. HELIQUEST: a web server to screen sequences with specific alpha-helical properties. *Bioinformatics* **2008**, 24 (18), 2101–2.
- (37) Rathinakumar, R.; Walkenhorst, W. F.; Wimley, W. C. Broad-spectrum antimicrobial peptides by rational combinatorial design and high-throughput screening: the importance of interfacial activity. *J. Am. Chem. Soc.* **2009**, 131 (22), 7609–17.
- (38) Zelezetsky, I.; Tossi, A. Alpha-helical antimicrobial peptides—using a sequence template to guide structure-activity relationship studies. *Biochim. Biophys. Acta* **2006**, 1758 (9), 1436–49.
- (39) Richardson, J. S.; Richardson, D. C. Amino acid preferences for specific locations at the ends of alpha helices. *Science* **1988**, 240 (4859), 1648–52.
- (40) Yang, P.; Ramamoorthy, A.; Chen, Z. Membrane orientation of MSI-78 measured by sum frequency generation vibrational spectroscopy. *Langmuir* **2011**, 27 (12), 7760–7.
- (41) Lee, D. K.; Brender, J. R.; Sciacca, M. F.; Krishnamoorthy, J.; Yu, C.; Ramamoorthy, A. Lipid composition-dependent membrane fragmentation and pore-forming mechanisms of membrane disruption by pexiganan (MSI-78). *Biochemistry* **2013**, 52 (19), 3254–63.
- (42) Hallock, K. J.; Lee, D. K.; Ramamoorthy, A. MSI-78, an analogue of the magainin antimicrobial peptides, disrupts lipid bilayer structure via positive curvature strain. *Biophys. J.* **2003**, 84 (5), 3052–60.
- (43) Wieprecht, T.; Dathe, M.; Beyermann, M.; Krause, E.; Maloy, W. L.; MacDonald, D. L.; Bienert, M. Peptide hydrophobicity controls the activity and selectivity of magainin 2 amide in interaction with membranes. *Biochemistry* **1997**, 36 (20), 6124–32.
- (44) Chen, Y.; Mant, C. T.; Farmer, S. W.; Hancock, R. E.; Vasil, M. L.; Hodges, R. S. Rational design of alpha-helical antimicrobial peptides with enhanced activities and specificity/therapeutic index. *J. Biol. Chem.* **2005**, 280 (13), 12316–29.
- (45) Chen, Y.; Guarnieri, M. T.; Vasil, A. I.; Vasil, M. L.; Mant, C. T.; Hodges, R. S. Role of peptide hydrophobicity in the mechanism of action of alpha-helical antimicrobial peptides. *Antimicrob. Agents Chemother.* **2007**, 51 (4), 1398–406.
- (46) Hawrani, A.; Howe, R. A.; Walsh, T. R.; Dempsey, C. E. Origin of low mammalian cell toxicity in a class of highly active antimicrobial amphipathic helical peptides. *J. Biol. Chem.* **2008**, 283 (27), 18636–45.
- (47) Hwang, H.; Hyun, S.; Kim, Y.; Yu, J. Reduction of helical content by insertion of a disulfide bond leads to an antimicrobial peptide with decreased hemolytic activity. *ChemMedChem* **2013**, 8 (1), 59–62.
- (48) Ramamoorthy, A. Beyond NMR spectra of antimicrobial peptides: dynamical images at atomic resolution and functional insights. *Solid State Nucl. Magn. Reson.* **2009**, 35 (4), 201–7.
- (49) Hoskin, D. W.; Ramamoorthy, A. Studies on anticancer activities of antimicrobial peptides. *Biochim. Biophys. Acta* **2008**, 1778 (2), 357–75.